ACKNOWLEDGMENT

The research presented in this paper was carried out when the author was staying at the Department of Electrical and Electronic Engineering, University of Nottingham, U.K., with the financial support of a fellowship from the Royal Society.

REFERENCES

[1] K. S. Yee, "Numerical solution of initial boundary value problems involving Maxwell's equations in isotropic media," *IEEE Trans. Antennas Propagat.*, vol. AP-14, pp. 302–307, May 1966.
[2] C. D. Taylor, D.-H. Lam, and T. H. Shumpert, "Electromagnetic pulse scattering in time-varying inhomogeneous media," *IEEE Trans. Antennas Propagat.*, vol. AP-17, pp. 585–589, Sept. 1969.
[3] A. Taflove and M. E. Brodwin, "Numerical solution of steady-state electromagnetic scattering problems using the time dependent Maxwell's equations," *IEEE Trans. Microwave Theory Tech.*, vol. MTT-23, pp. 623–630, Aug. 1975.
[4] D. E. Merewether, "Transient currents induced on a metallic body of revolution by an electromagnetic pulse," *IEEE Trans. Electromagn. Compat.*, vol. EMC-13, pp. 41–44, May 1971.
[5] K. S. Kunz and K.-M. Lee, "A three-dimensional finite-difference solution of the external response of an aircraft to a complex transient EM environment: Part I—The method and its implementation." *IEEE Trans. Electromagn. Compat.*, vol. EMC-20, pp. 328–333, May 1978.
[6] A. Taflove, "Application of the finite-difference time-domain method to sinusoidal steady-state electromagnetic penetration problems," *IEEE Trans. Electromagn. Compat.*, vol. EMC-22, pp. 191–202, 1980.
[7] R. Holland, L. Simpson, and K. S. Kunz, "Finite-difference analysis of EMP coupling to lossy dielectric structures," *IEEE Trans. Electromagn. Compat.*, vol. EMC-22, pp. 203–209, 1980.
[8] D. S. Jones, *The Theory of Electromagnetism.* Oxford, England: Pergamon, 1964, p. 566.
[9] G. Mur, "Absorbing boundary conditions for the finite-difference approximation of the time-domain electromagnetic-field equations," submitted for publication.

Gerrit Mur was born on February 16, 1942, in Laag-Nieuwkoop, the Netherlands. After graduating from a polytechnic in Utrecht in 1963 he obtained the masters degree in electrical engineering in 1970 and the Ph.D. degree in 1978, both from the Delft University of Technology, Delft, The Netherlands.

From 1970 he worked as a lecturer at the Department of Electrical Engineering of Delft University, and since 1978 he has been a Senior Lecturer. His main research interest is in the development and application of numerical methods for computing electromagnetic fields in complicated geometries.

Coupled-Mode Theory Analysis of Distributed Nonreciprocal Structures

IKUO AWAI, MEMBER, IEEE, AND TATSUO ITOH, SENIOR MEMBER, IEEE

***Abstract*—A general coupled-mode theory is developed for dielectric waveguide structures containing a gyrotropic layer. The theory is applied to several specific structures. Based on qualitative and numerical analyses, we studied the feasibility of such structures as the new type of nonreciprocal devices for millimeter-wave applications. A number of considerations for practical designs are included.**

Manuscript received March 27, 1981; revised June 3, 1981. This work was supported by ONR under Contract N00014-C-0553 and in part under a Joint Services Electronics Program F49620-77-C-0101. The major portion of this paper was presented at the 1981 International Microwave Symposium.

I. Awai was with the Department of Electrical Engineering, University of Texas, Austin, TX 78712. He is now with the Department of Electronic Engineering, Kyoto University, Kyoto, Japan.

T. Itoh is with the Department of Electrical Engineering, University of Texas, Austin, TX 78712.

I. INTRODUCTION

DEVELOPMENT of microwave and millimeter-wave isolators and circulators becomes more difficult as the frequency is increased [1], [2]. This is because the nonreciprocal property of ferrite used for these devices represented by the ratio of off-diagonal and diagonal components of the permeability tensor decreases with the frequency. One solution is to use a ferrite with high-saturation magnetization ($4\pi M$). However, it is difficult to obtain a ferrite material with more than 5 kG of $4\pi M$.

0018-9480/81/1000-1077$00.75 ©1981 IEEE

Another problem is high dielectric and magnetic losses in the ferrite materials at millimeter-wave frequencies. Therefore, it is extremely difficult to create a conventionally designed isolator or circulator with a low insertion loss at frequencies above 150 GHz.

We propose here a new type of nonreciprocal device and analyze it based on the mode-coupling technique frequently employed in integrated optics. It was found that the propagation constants of a ferrite waveguide can be made different for the waves propagating in the opposite direction if a static magnetic field is properly applied [3]. Consider the case in which a ferrite waveguide is placed in parallel near a low-loss dielectric waveguide.

If the propagation constant in the dielectric waveguide is made different from that of the wave in the ferrite guide propagating in the forward direction and identical to that in the latter propagating in the backward direction, the energy in the dielectric waveguide does not couple into the ferrite guide for the forward propagation, whereas the energy is transferred into the ferrite guide for the backward propagation. Since we use the low-loss dielectric waveguide as the main guide, we could realize low forward insertion loss and, at the same time, high backward isolation in this arrangement. A circulator may be realized by using all four arms of the coupled structure as discussed later. Our discussions, however, will be mostly on the isolator structure and only basic concepts for realizing a circulator will be given.

If the available ferrite material is very lossy, the ferrite guide itself can be used as an absorber, and hence, we do not need terminations for the ferrite guide nor tapered access of two guides as in a conventional directional coupler. We will examine this case in a separate section later.

If we can obtain a ferrite of very low loss, while the saturation magnetization is not large enough to be used for the nonreciprocal guide, we can use it in place of the dielectric waveguide. This arrangement results in the same low forward insertion loss. This topic will also be discussed later.

In the next section, we present a general coupled-mode theory for the structure continuing a gyrotropic medium. In Section III, we perform a qualitative study based on the assumption that the coupling is vanishingly small. Section IV introduces specific coupling structures to be used for proposed isolators. Numerical studies for the proposed structures are undertaken in Section V. A method for creating a circulator will also be discussed. A modified form of isolators with a built-in absorptive loss is discussed in Section VI.

II. Perturbation and Coupled-Mode Theory

Let us assume that the coupling of two guides is relatively weak. Therefore, we can use a perturbation method, taking each guide without the other as the basis structure. Marcuse has developed a coupled-mode theory for anisotropic waveguides [4]. In the present paper, his theory is extended to the cases where gyrotropic materials, such as ferrite, are involved. We will assume that the coupling is only between two guided modes of each waveguide. The modal field in each basis structure ($i=1,2$) satisfies the following Maxwell's equation:

$$\nabla_t \times \bar{E}_i - j\beta_i \hat{a}_y \times \bar{E}_i = -j\omega \bar{\bar{\mu}}_i \cdot \bar{H}_i$$
$$\nabla_t \times \bar{H}_i - j\beta_i \hat{a}_y \times \bar{H}_i = j\omega \bar{\bar{\epsilon}}_i \bar{E}_i \qquad (i=1,2) \qquad (1)$$

where ∇_t signifies the transverse derivative, β_i the propagation constant of each mode, and $\bar{\bar{\mu}}_i$ and $\bar{\bar{\epsilon}}_i$ are permeability and permittivity tensor for each guide, respectively, and are functions of position in each structure. These tensor quantities allow us to handle the cases where both guides are anisotropic or gyrotropic. In addition, we assume the propagation is along the y-direction. The electric and magnetic fields are proportional to $e^{j\omega t}$ and this term is suppressed for simplicity. The direction of the dc magnetic field is taken as the z-direction.

According to the perturbation theory, the coupled field is written as a linear combination of modal fields in two basis structures

$$\bar{E} = c_1 \bar{E}_1 + c_2 \bar{E}_2$$
$$\bar{H} = c_1 \bar{H}_1 + c_2 \bar{H}_2. \qquad (2)$$

Substituting (2) into Maxwell's equation for the coupled structure, we obtain the following two relations:

$$\left(\frac{\partial c_1}{\partial y} + j\beta_1 c_1\right)\hat{a}_y \times \bar{E}_1 + \left(\frac{\partial c_2}{\partial y} + j\beta_2 c_2\right)\hat{a}_y \times \bar{E}_2 = -j\omega\left[\left(\bar{\bar{\mu}} - \bar{\bar{\mu}}_1\right)\cdot c_1 \bar{H}_1 + \left(\bar{\bar{\mu}} - \bar{\bar{\mu}}_2\right)\cdot c_2 \bar{H}_2\right] \qquad (3)$$

$$\left(\frac{\partial c_1}{\partial y} + j\beta_1 c_1\right)\hat{a}_y \times \bar{H}_1 + \left(\frac{\partial c_2}{\partial y} + j\beta_2 c_2\right)\hat{a}_y \times \bar{H}_2 = j\omega\left[\left(\bar{\bar{\epsilon}} - \bar{\bar{\epsilon}}_1\right)\cdot c_1 \bar{E}_1 + \left(\bar{\bar{\epsilon}} - \bar{\bar{\epsilon}}_2\right)\cdot c_2 \bar{E}_2\right] \qquad (4)$$

where $\bar{\bar{\epsilon}}$ and $\bar{\bar{\mu}}$ are tensor permittivity and permeability of the coupled structure and are once again functions of position.

Multiplying (3) and (4) by $\bar{H}_1^*$ and $\bar{E}_1^*$, respectively, integrating over the cross section of the guides, and taking difference of the resultant equations, we obtain

$$\left(D_{11}\cdot\frac{\partial}{\partial y} + jN_{11}\right)c_1 + \left(D_{12}\frac{\partial}{\partial y} + jN_{12}\right)c_2 = 0 \qquad (5)$$

where

$$D_{11} = \int\left[\bar{H}_1^*\cdot\left(\hat{a}_y \times \bar{E}_1\right) - \bar{E}_1^*\cdot\left(\hat{a}_y \times \bar{H}_1\right)\right] dS$$
$$= \int \hat{a}_y \cdot \left(\bar{E}_1 \times \bar{H}_1^* + \bar{E}_1^* \times \bar{H}_1\right) dS$$

$$D_{12} = \int\left[\bar{H}_1^*\cdot\left(\hat{a}_y \times \bar{E}_2\right) - \bar{E}_1^*\cdot\left(\hat{a}_y \times \bar{H}_2\right)\right] dS$$
$$= \int \hat{a}_y \cdot \left(\bar{E}_2 \times \bar{H}_1^* + \bar{E}_1^* \times \bar{H}_2\right) dS$$

$$N_{11} = \beta_1 D_{11} + \omega\int\left[\bar{H}_1^*\cdot\left(\bar{\bar{\mu}} - \bar{\bar{\mu}}_1\right)\cdot\bar{H}_1 + \bar{E}_1^*\cdot\left(\bar{\bar{\epsilon}} - \bar{\bar{\epsilon}}_1\right)\cdot\bar{E}_1\right] dS$$

$$N_{12} = \beta_2 D_{12} + \omega\int\left[\bar{H}_1^*\cdot\left(\bar{\bar{\mu}} - \bar{\bar{\mu}}_2\right)\cdot\bar{H}_2 + \bar{E}_1^*\cdot\left(\bar{\bar{\epsilon}} - \bar{\bar{\epsilon}}_2\right)\cdot\bar{E}_2\right] dS. \qquad (6)$$

Here, the integrations are over the waveguide cross sections. In a similar manner, we get

$$\left(D_{21}\frac{\partial}{\partial y}+jN_{21}\right)c_1+\left(D_{22}\frac{\partial}{\partial y}+jN_{22}\right)c_2=0 \tag{7}$$

where

$$D_{21}=\int \hat{a}_y\cdot\left(\bar{E}_1\times\bar{H}_2^*+\bar{E}_2^*\times\bar{H}_1\right)dS$$

$$D_{22}=\int \hat{a}_y\cdot\left(\bar{E}_2\times\bar{H}_2^*+\bar{E}_2^*\times\bar{H}_2\right)dS$$

$$N_{21}=\beta_1 D_{21}+\omega\int\left[\bar{H}_2^*\cdot\left(\bar{\bar{\mu}}-\bar{\bar{\mu}}_1\right)\cdot\bar{H}_1+\bar{E}_2^*\cdot\left(\bar{\bar{\epsilon}}-\bar{\bar{\epsilon}}_1\right)\cdot\bar{E}_1\right]dS$$

$$N_{22}=\beta_2 D_{22}+\omega\int\left[\bar{H}_2^*\cdot\left(\bar{\bar{\mu}}-\bar{\bar{\mu}}_2\right)\cdot\bar{H}_2+\bar{E}_2^*\cdot\left(\bar{\bar{\epsilon}}-\bar{\bar{\epsilon}}_2\right)\cdot\bar{E}_2\right]dS. \tag{8}$$

The quantities D_{11} and D_{22} are four times the Poynting energy of the unperturbed waveguides. D_{12} and D_{21} represent the cross integrals of the two modes, which become zero if they are orthogonal to each other. The symmetry property of D_{ij} and N_{ij} is examined in the Appendix.

If we write $c_1=C_1e^{-jky}$ and $c_2=C_2e^{-jky}$ where k is the propagation constant of the coupled structure, (5) and (7) are reduced to

$$\left[\begin{pmatrix}N_{11}&N_{12}\\N_{21}&N_{22}\end{pmatrix}-k\begin{pmatrix}D_{11}&D_{12}\\D_{21}&D_{22}\end{pmatrix}\right]\begin{pmatrix}C_1\\C_2\end{pmatrix}=0 \tag{9}$$

in a matrix representation. The propagation constant k of the coupled mode is given by equating the determinant of the coefficient matrix of (9) to zero.

$$k_{12}=\frac{D_{11}N_{22}+D_{22}N_{11}-(D_{12}N_{21}+D_{21}N_{12})\pm\sqrt{\{(D_{11}N_{22}+D_{22}N_{11})-(D_{12}N_{21}+D_{21}N_{12})\}^2-4(D_{11}D_{22}-D_{12}D_{21})\times(N_{11}N_{22}-N_{12}N_{21})}}{2(D_{11}D_{22}-D_{12}D_{21})}. \tag{10}$$

Substituting (10) into (9), we know the ratio of C_1 and C_2. Since we have two solutions for k, namely k_1 and k_2, there are two sets of (C_1, C_2). For k_1, we write the solution as $(C_1^{(1)}, C_2^{(1)})$ whereas $(C_1^{(2)}, C_2^{(2)})$ is for k_2. Therefore, the coupled field $\bar{E}$ in (2) also has two solutions.

$$\bar{E}^{(1)}=\left[C_1^{(1)}\bar{E}_1+C_2^{(1)}\bar{E}_2\right]e^{-jk_1y}$$
$$\bar{E}^{(2)}=\left[C_1^{(2)}\bar{E}_1+C_2^{(2)}\bar{E}_2\right]e^{-jk_2y}. \tag{11}$$

Generally, a mixture of $\bar{E}^{(1)}$ and $\bar{E}^{(2)}$ exists in the coupled structure. Therefore, the fields $\bar{e}_1$ and $\bar{e}_2$ principally associated with the basis structures 1 and 2, respectively, may be expressed as

$$\bar{e}_1(y)=\bar{E}_1\left[AC_1^{(1)}e^{-jk_1y}+BC_1^{(2)}e^{-jk_2y}\right]$$
$$\bar{e}_2(y)=\bar{E}_2\left[m_1AC_1^{(1)}e^{-jk_1y}+m_2BC_1^{(2)}e^{-jk_2y}\right] \tag{12}$$

where $m_1=C_2^{(1)}/C_1^{(1)}$ and $m_2=C_2^{(2)}/C_1^{(2)}$ are given by

$$m_i=-\frac{N_{11}-k_iD_{11}}{N_{12}-k_iD_{12}}\qquad(i=1,2). \tag{13}$$

A and B are determined by the initial condition.

If we assume the wave is incident only in Guide 1, the electric fields of the two guides are calculated as

$$\bar{e}_1(y)=\frac{1}{m_2-m_1}\left(m_2e^{-jk_1y}-m_1e^{-jk_2y}\right)\bar{E}_1$$
$$\bar{e}_2(y)=\frac{m_1m_2}{m_2-m_1}\left(e^{-jk_1y}-e^{-jk_2y}\right)\bar{E}_2. \tag{14}$$

III. Energy Exchange Between Two Waveguides

Before going to numerical studies for specific structures based on the theory previously developed, one finds it useful to investigate the qualitative nature of the mode-coupling phenomena. To this end, we further simplify the model by temporarily assuming the cross integral D_{ij} $(i\neq j)$ is zero. This is a realistic approximation since, in many coupled structures, D_{ij} is relatively small due to weak coupling of two basis structures.

Since N_{ij}/D_{ij} has a dimension of propagation constant, we write

$$N_{11}/D_{11}=\beta_1-j\alpha_1$$
$$N_{12}/D_{11}=N_{21}/D_{22}=\kappa$$
$$N_{22}/D_{22}=\beta_2-j\alpha_2\quad\text{or}\quad\beta_2'-j\alpha_2'$$

where α_i, β_i, and κ are all real positive quantities. Here, we introduced attenuation α_i to account for the loss in each waveguide. Thus we have a mode-coupling containing losses illustrated in Fig. 1. We assume that Guide 1 is a conventional dielectric waveguide and Guide 2 is made of a gyrotropic medium. Notice that the propagation constants for forward and backward directions are different in the nonreciprocal Guide 2.

It is well known [5] that the main properties of mode coupling are described by such quantities as $(\beta_1-\beta_2)/\kappa$ and $(\alpha_1-\alpha_2)/\kappa$. However, we equate α_1 to zero, and deal with $(\beta_1-\beta_2)/\kappa$ and α_2/κ instead because α_1 is small, anyway, in a typical dielectric waveguide. In this way, we can avoid the trivial effect of small α_1, which decreases the energy carried by both guides almost equally.

Fig. 2 shows the amplitude of the wave in each waveguide versus propagation distance. The loss parameter α_2 here is made rather small. Hence, the energy initiated in Guide 1 is exchanged between two guides without noticeable dissipation.

One of the most important features in Fig. 2 is that the energy exchange rate depends strongly on $|\beta_1-\beta_2|$. If we make $|\beta_1-\beta_2|/\kappa$ larger for the forward propagation, there is little coupling between the forward propagating wave in Guide 1 and the one in Guide 2. On the other hand, we can increase coupling between the backward propagating wave in Guide 1 and the one in Guide 2 by making this quantity small. In this way, we can realize nonreciprocal energy exchange as long as the coupling length is properly selected.

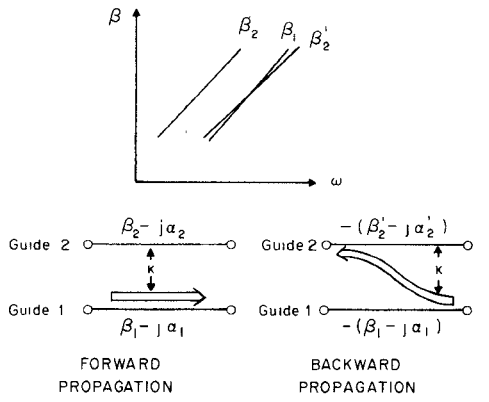

Fig. 1. The principle of the proposed isolator.

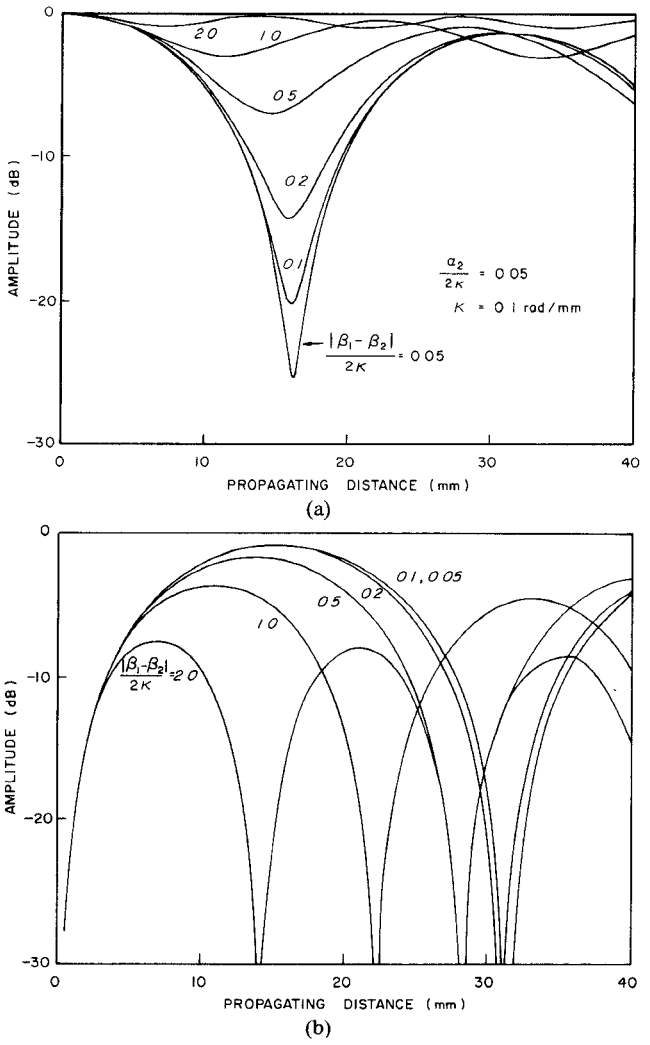

Fig. 2. (a)The wave amplitude of Guide 1 versus propagating distance for the low-loss case. (b)The wave amplitude of Guide 2 versus propagating distance for the low-loss case.

The potential deficiency in this mechanism for an isolator is that we have to bring the energy in the Guide 2 out carefully from the coupling region by a tapered section followed by a matched load for the backward propagation. Otherwise, this energy is reflected at the terminals of Guide 2 and coupled back to Guide 1 and deteriorates the isolation characteristics.

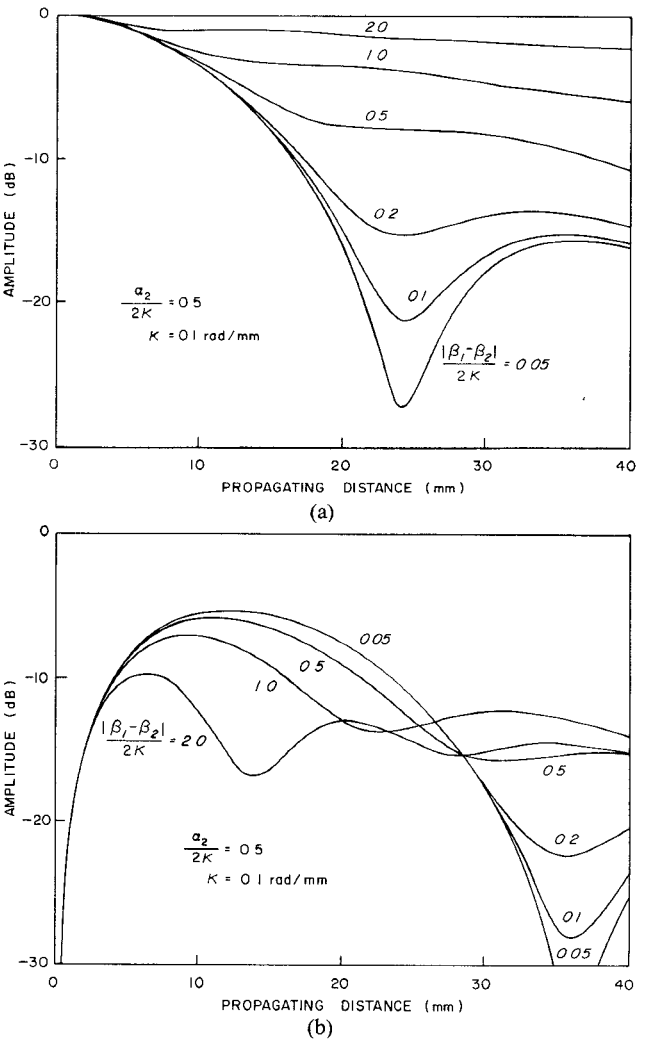

Fig. 3. (a)The wave amplitude of Guide 1 versus propagating distance for the high-loss case. (b)The wave amplitude of Guide 2 versus propagating distance for the high-loss case.

There is, however, a possible way to avoid this phenomenon. Most ferrites are relatively lossy at millimeter-wave frequencies. We can make use of this type of ferrite for the guide and the absorber at the same time. Fig. 3 illustrates the mode-coupling property for large α_2. When $|\beta_1-\beta_2|/\kappa$ is small, the energy in Guide 1 goes into Guide 2 because of strong coupling and is dissipated. Hence, neither matched loads nor tapered sections are necessary for absorbing the unwanted signal. One can use a truncated ferrite guide alongside the dielectric main guide. However, the forward propagation loss (the insertion loss) becomes greater due to a greater ferrite loss. Therefore, we need larger nonreciprocity ($|\beta_2'-\beta_2|/\kappa$) to reduce the insertion loss.

IV. Basis Structures

In this section, we select specific structures useful for millimeter-wave application and introduce characteristic quantities necessary for studying nonreciprocal phenomena. Although, in practice, a three-dimensional structure, e.g., microstrip or image guide, etc., is used for integrated circuit, we will employ a two-dimensional planar structure for simplicity of analysis. Fundamental properties of the

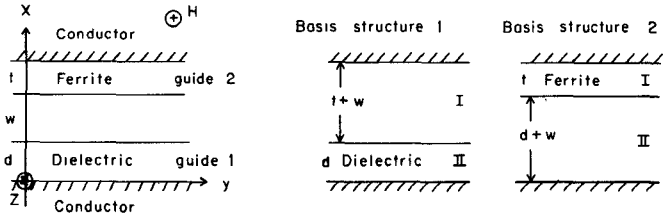

Fig. 4. Calculated structure and two basis structures.

coupled-mode isolator are still preserved in a two-dimensional structure.

Recently, it was shown that a planar waveguide containing ferrite exhibits maximum nonreciprocity in the propagation constant, i.e., $|\beta^+ - \beta^-|$ becomes maximum, when it has a dielectric–ferrite–metal structure [6]. We will, however, take a simpler ferrite–metal structure (metal-backed ferrite plate) which still has reasonably large nonreciprocity. As for the main guide, we may choose a dielectric slab. However, we have chosen a metal-backed dielectric slab which simulates an image guide often employed in many millimeter-wave circuits.

The structure to be analyzed is shown in Fig. 4. Also indicated are the two basis structures used in the coupled-mode theory. The quantities necessary for calculating (14) will be shown in the following.

A. Basis Structure 1 (Dielectric Waveguide)

Field components are

$$\text{Region I}\begin{cases} E_z = \dfrac{a\sin\zeta d}{\sinh\xi(t+w)}\sinh\xi(t+d+w-x) \\ H_x = \dfrac{a\beta_1}{\omega\mu_0}E_z \\ H_y = \dfrac{ja\xi}{\omega\mu_0}\dfrac{\sin\zeta d}{\sinh\xi(t+w)}\cosh\xi(t+d+w-x) \end{cases} \tag{15}$$

$$\text{Region II}\begin{cases} E_z = a\sin\zeta x \\ H_x = \dfrac{a\beta_1}{\omega\mu_0}E_z \\ H_y = -\dfrac{ja\zeta}{\omega\mu_0}\cos\zeta x \end{cases} \tag{16}$$

where a is the amplitude coefficient.

The dispersion relation for this structure is

$$\zeta\tanh\xi(t+w)+\xi\tan\zeta d=0 \tag{17}$$

and the Poynting energy P_1 is given by

$$P_1=\frac{a^2\beta_1}{4\omega\mu_0}\left[d-\frac{\sin 2\zeta d}{2\zeta}+\frac{\sin^2\zeta d}{\xi\sinh^2\xi(t+w)}\cdot\left\{\frac{\sinh 2\xi(t+w)}{2}-\xi(t+w)\right\}\right] \tag{18}$$

where

$$\zeta=\sqrt{k_0^2\epsilon_d-\beta_1^2}\qquad \xi=\sqrt{\beta_1^2-k_0^2\epsilon_g}. \tag{19}$$

$k_0=\sqrt{\omega^2\epsilon_0\mu_0}$ is the propagation constant in free space, ϵ_d is the relative dielectric constant of the dielectric plate, and ϵ_g is that of the gap between the dielectric and the upper conductor.

B. Basis Structure 2 (Ferrite Waveguide)

Field components are

$$\text{Region I}\begin{cases} E_z = b\sin\eta(t+d+w-x) \\ H_x = \dfrac{b}{\omega\mu_0\mu_e}\{\beta_2\sin\eta(t+d+w-x) \\ \qquad +\sigma\eta\cos\eta(t+d+w-x)\} \\ H_y = \dfrac{jb}{\omega\mu_0\mu_e}\{\sigma\beta_2\sin\eta(t+d+w-x) \\ \qquad +\eta\cos\eta(t+d+w-x)\} \end{cases} \tag{20}$$

$$\text{Region II}\begin{cases} E_z = \dfrac{b\sin\eta t}{\sinh\theta(d+w)}\sinh\theta x \\ H_x = \dfrac{b\beta_2}{\omega\mu_0}E_z \\ H_y = -\dfrac{jb\theta}{\omega\mu_0}\dfrac{\sin\eta t}{\sinh\theta(d+w)}\cosh\theta x \end{cases} \tag{21}$$

where b is the amplitude factor.

Dispersion relation

$$(\sigma\beta_2\tan\eta t+\eta)\tanh\theta(d+w)+\mu_e\theta\tan\eta t=0. \tag{22}$$

Poynting energy

$$P_2=\frac{b^2\beta_2}{4\omega\mu_0\mu_e}\left[t-\frac{\sin 2\eta t}{2\eta}+\frac{\sigma}{\beta_2}\sin^2\eta t+\frac{\mu_e\sin^2\eta t}{\theta\sinh^2\theta(d+w)}\left\{\frac{\sinh 2\theta(d+w)}{2}-\theta(d+w)\right\}\right] \tag{23}$$

where

$$\eta=\sqrt{k_0^2\epsilon_m\mu_e-\beta_2^2}\qquad \theta=\sqrt{\beta_2^2-k_0^2\epsilon_g}. \tag{24}$$

ϵ_m is the relative dielectric constant of the ferrite, μ_e is the effective permeability given by [17]

$$\mu_e=\frac{\omega^2-\omega_s^2}{\omega^2-\omega_B^2}=\frac{\omega^2-\gamma^2(H+4\pi M)^2}{\omega^2-\gamma^2H(H+4\pi M)} \tag{25}$$

γ gyromagnetic ratio
$4\pi M$ saturation magnetization
H applied static magnetic field

and σ is the ratio of the off-diagonal and diagonal parts of the permeability tensor

$$\sigma=\frac{\nu}{\mu}=\frac{\omega\gamma 4\pi M}{\omega^2-\gamma^2H(H+4\pi M)}. \tag{26}$$

The dc magnetic field is applied in the z-direction.

If material losses are taken into account, we need to introduce the following substitutions in (7) and (9):

$$\begin{aligned} \epsilon_d &\to \epsilon_d' - j\epsilon_d'' \\ \epsilon_m &\to \epsilon_m' - j\epsilon_m'' \\ \epsilon_g &\to \epsilon_g' - j\epsilon_g'' \\ H &\to H + j\Delta H \end{aligned} \tag{27}$$

where ΔH is called a resonance linewidth of a ferrite. The conductor loss is accounted for in the following way. In the derivation of the dispersion relation for the basis structures, we assume finite conductivity in the metal and obtain complex propagation constants. They are used as β_1 and β_2 in N_{ij} in (6) and (8). However, the field components need not be modified as long as the imaginary part of β is small.

V. Coupled-Mode Isolator and Circulator

Usually, microwave ferrites have a large relative dielectric constant, i.e., 8 to 16. Therefore, the dielectric used as the main guide should have a comparable value to realize phase matching with the ferrite guide. Once the dielectric constant is determined, the thickness of the dielectric d is chosen so as to allow only the fundamental mode to propagate. Then, the thickness of the ferrite t is determined to give a phase matching at the operating frequency.

Since it is desirable to have the widest possible operating bandwidth for the isolator, the careful matching of the propagation constants for two waveguides would be needed in the beginning of the synthesis. It may not be enough to make these propagation constants degenerate at one frequency point. Rather, it would be necessary to have $\partial\beta/\partial\omega$ equal at the same time or even to try a least square method for certain frequency ranges. It turns out, however, that these procedures are unnecessary, because one of the factors restricting the bandwidth, viz., the coupling coefficient, unfortunately ruins the result of the deliberate matching. Hence, we will choose here the parameters simply by a trial and error for which good matching is obtainable, as is shown in Fig. 5.

The next step is to determine the separating distance w between two guides. If w is too small, the coupling coefficient κ becomes too large not only for the backward but also for the forward propagation, and the forward attenuation becomes excessively large. We recognize that when $|\beta_1-\beta_2|/\kappa$ is small, the attenuation becomes large, as shown in Fig. 2. On the other hand, if two guides are separated too much, the coupling length becomes too long, resulting in large attenuation due to the dielectric and conductor loss in the main guide. Hence, there is an optimum separation which compromises the above two situations.

Calculating (14) with the parameters listed in Fig. 5, we can obtain the signal amplitude variation versus the propagating distance for the two guides, as shown in Fig. 6. The lower the frequency, the smaller the transverse propagation constant is; i.e., we have the slower transverse field decay which makes the coupling between the two basis modes stronger and the coupling length[1] shorter. This is the reason it is of no use to attempt a precise propagation constant matching between the backward-propagating modes for a wide frequency range. If the transverse-propagation constant did not change with the frequency, we could have the constant coupling length and have a far better frequency characteristic for the isolator.

Even when the bandwidth is narrow, this structure is still

[1]By the phrase "coupling length" we mean the distance between the two neighboring peaks in Fig. 6.

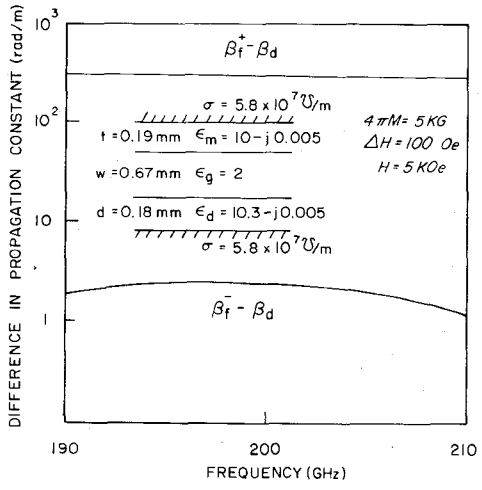

Fig. 5. Parameters employed in the calculation and the difference of propagation constants between the two basis structures for the forward and backward propagation direction.

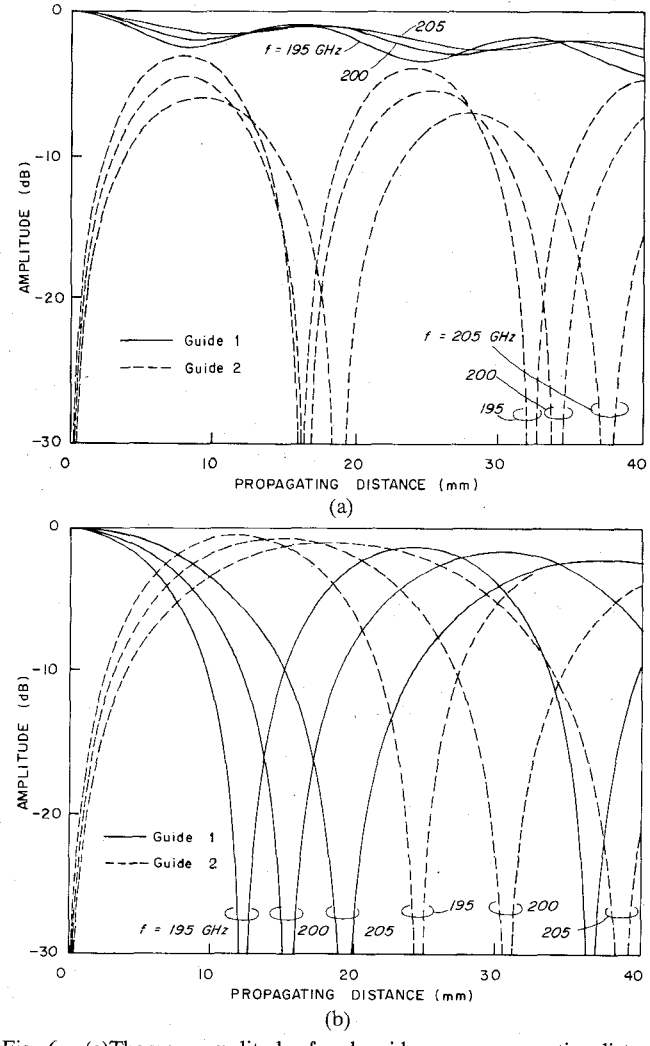

Fig. 6. (a)The wave amplitude of each guide versus propagating distance for the forward direction. (b)The wave amplitude of each guide versus propagating distance for the backward direction.

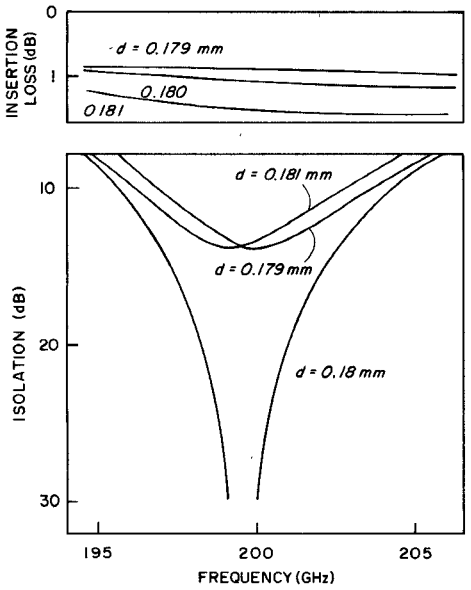

Fig. 7. The frequency characteristic of the forward-insertion loss and the backward isolation for a coupled-mode isolator and its tolerance with the dielectric thickness d.

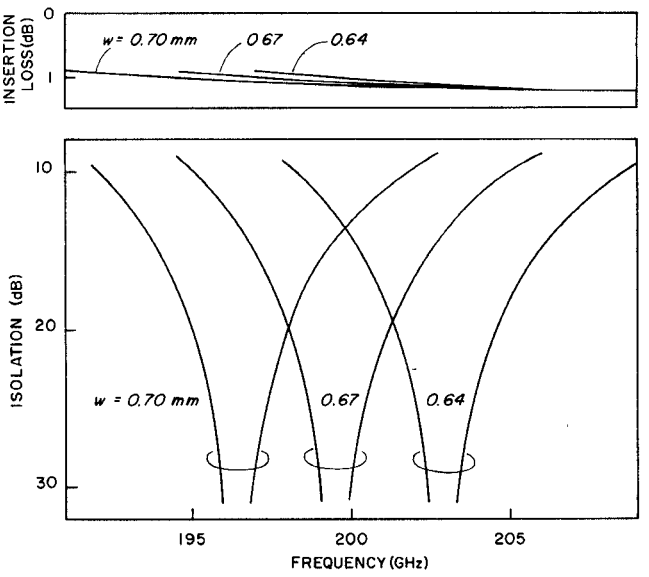

Fig. 8. The tolerance of the gap width w.

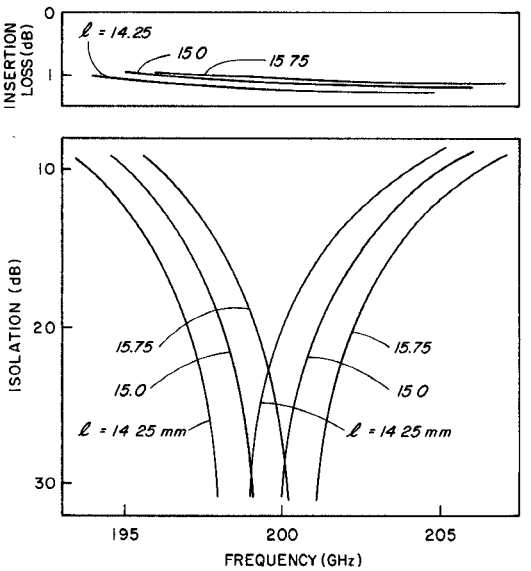

Fig. 9. The tolerance of the length of coupling l.

promising as long as the forward attenuation is low. We will proceed further by setting the length of coupling[2] to an adequate value, e.g., 15 mm. This choice has been made in order to have minimum forward and maximum backward attenuation around 200 GHz with 0.67 mm distance between the two guides. The insertion loss is around 1 dB and the 10-dB-isolation bandwidth is 10 GHz for this case (Fig. 7). This figure gives the typical and realizable characteristics of the proposed isolator, since the parameters assumed are reasonable, considering the state of art on the materials.

Now, starting with these parameters, we will examine hereafter other important properties, especially the tolerance of fabrication. Remembering that this is a coupled-mode-type device, we speculate that the thickness control might be the most severe. Suppose the dielectric constants ϵ_d and ϵ_m of two materials and the thickness t of the ferrite are given, the forward and backward attenuation are shown in Fig. 7 with the thickness d of the dielectric shifted a little from the optimum value (0.18 mm). In fact, only 0.5-percent deviation makes the isolation noticeably worse. This deterioration may be relieved by tuning with the applied magnetic field, though the tuning range is not very wide. The other parameters are not so critical as above. The gap width w and the length of coupling l is changed around ± 5 percent from the optimum value in Figs. 8 and 9, respectively. The effect is mainly the shift of center frequency for the backward isolation and the forward loss is not affected very much.

The tolerance required of ϵ_d, ϵ_m, or $4\pi M$ is not expected to be critical because these parameters come into the dispersion relation with a square root, as shown in (19) or (24). Another interesting phenomenon to be examined is how small a value of ϵ_d can be used without noticeable degradation of isolator characteristics. If a dielectric with lower permittivity is used, the forward loss of the isolator will be reduced, as such a material usually has a lower loss tangent. Fig. 10 shows the result for $\epsilon_d = 8$ and 6 with an identical imaginary part, as in Fig. 5. The thickness of each material has been set to have a degeneracy of propagation constant at around 200 GHz. The 10-dB-isolation bandwidth is seen to decrease by 15 percent every time the dielectric constant is decreased by two. This is obviously because the dispersion curves for the dielectric and ferrite guides intersect with a larger angle, resulting in a larger mismatch of propagation constants for the backward propagation. The insertion loss also decreases at the lower edge of the operating band, while it increases at the upper edge.

Let us now turn our attention to the distributed circulator based on the mode coupling (see Fig. 11). The power

[2]The phrase "length of coupling" means the length where the interaction between the two guides takes place.

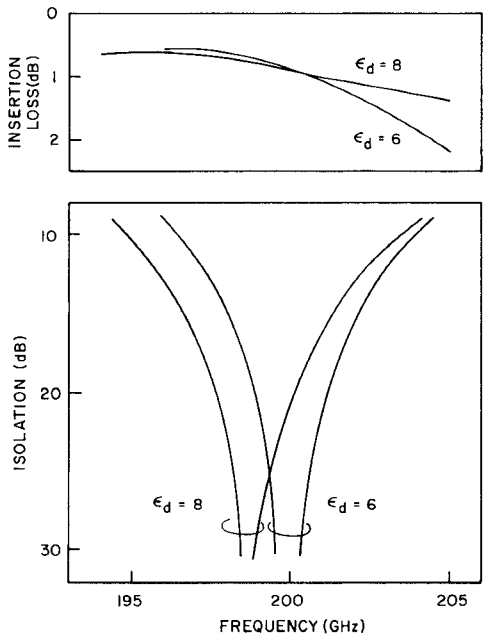

Fig. 10. The frequency characteristic of the forward-insertion loss and the backward isolation for lower dielectric constants in the main guide.

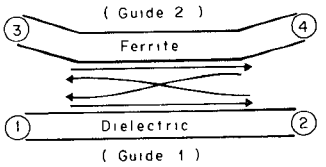

Fig. 11. Circulator operation of the coupled-mode isolator.

incident at port 1 of Guide 1 (main guide made of a dielectric) can be designed to pass to port 2 without much coupling to Guide 2 (ferrite guide), whereas the power from port 2 couples to Guide 2, as we discussed above, for realizing an isolator. The power injected at port 3 obviously does not couple to Guide 1 and is brought to port 4 without much attenuation if the ferrite loss is small. On the other hand, the power from port 4 couples to Guide 1 as the phase velocity for this wave in the ferrite guide is chosen to be close to that in Guide 1. As shown in Fig. 11, this device can be used as a circulator.

VI. Absorptive Coupled-Mode Isolator and Double-Ferrite Isolator

If the ferrite guide is very lossy, the power transferred from the main guide attenuates rapidly, and hence, an abrupt truncation of ferrite guide would not cause a serious problem for the isolation property as was stated before. Examples of the energy carried by each guide are shown in Fig. 12 with propagating distance both for the forward and backward directions. With those parameters shown in the figure, the widest band is obtained for the structure with 35 mm of the length of coupling, where the power in the ferrite guide for the backward propagation is less than -6 dB for 195–205 GHz. Therefore, as is shown in Fig. 13, the abrupt ends will cause roughly less than -14-dB leakage power assuming complete reflection at each end of the ferrite guide. This is added to the feedthrough power

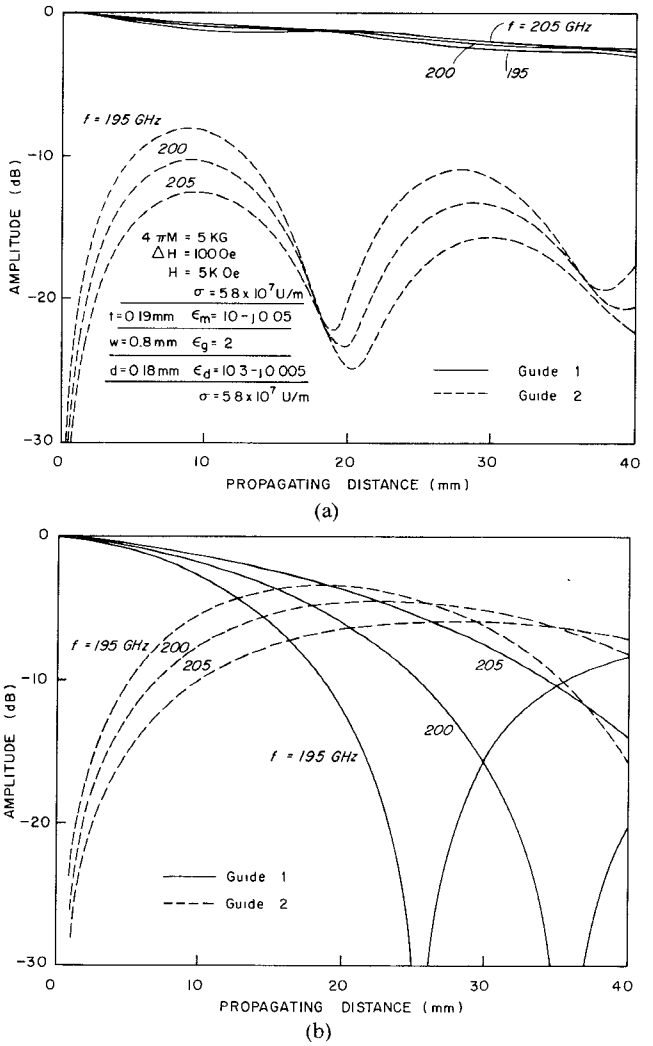

Fig. 12. (a)The parameters employed in the calculation of an absorptive coupled-mode isolator and the amplitude of each guide versus propagating distance for the forward direction. (b)The wave amplitude of each guide versus propagating distance for the backward direction.

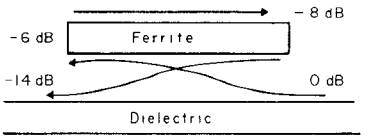

Fig. 13. The effect of truncation of the ferrite guide.

shown by solid lines in Fig. 12(b). The performance is expected to be better in a practical structure, because no complete reflections occur at the truncated ends of the ferrite. The frequency characteristic of this isolator is shown in Fig. 14. We can see that the forward-insertion loss is increased compared with Fig. 7.

It will be appropriate to analyze the forward-loss mechanism here. Because of the coupling between two guides, it is difficult to distinguish the origins of the insertion loss exactly. However, since most of the power stays in the main guide for the forward propagation, the signal experiences the effect of the loss tangent of the dielectric and the finite conductivity of the underlying metal almost constantly. Hence, we can obtain some estimates of each

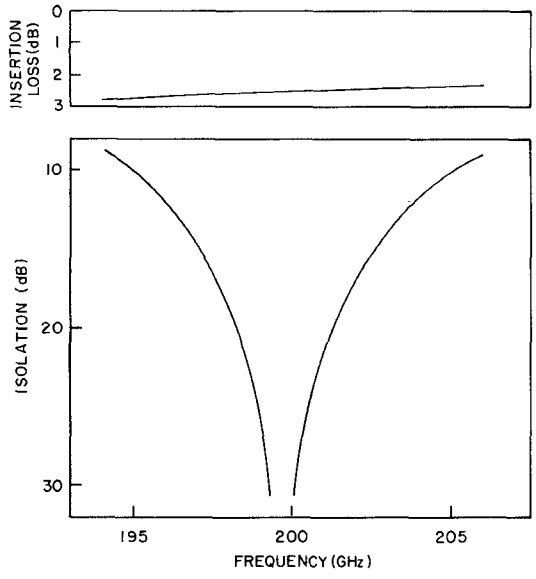

Fig. 14. The frequency characteristic of the forward-insertion loss and the backward isolation for an absorptive coupled-mode isolator (l=35 mm).

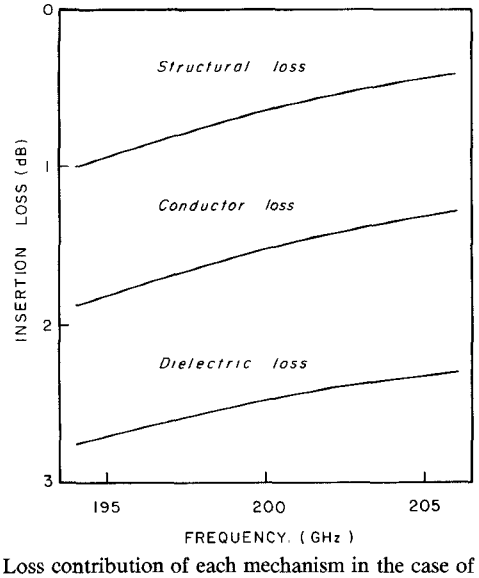

Fig. 15. Loss contribution of each mechanism in the case of an absorptive coupled-mode isolator.

contribution by making the loss tangent of the dielectric zero and the conductivity of the metal infinity, respectively. Fig. 15 shows the computed results. The "structural loss" is mainly composed of the magnetic and dielectric loss of the ferrite guide, but it also includes the interaction effect of each loss mechanism. As a result of the relatively large length (35 mm) of coupling, the loss from the main guide is rather high. On the contrary, we can expect a significant reduction of loss if we can afford a better dielectric with low loss and/or if we can do without the underlying metal. The conductor loss of around 1 dB may be taken off by making use of a single dielectric line instead of the image line as the main guide.

If a ferrite material, which has a low-loss tangent but not enough saturation magnetization is available, such a material can be used in place of the dielectric in the main guide. Because of the asymmetry of the structure, the

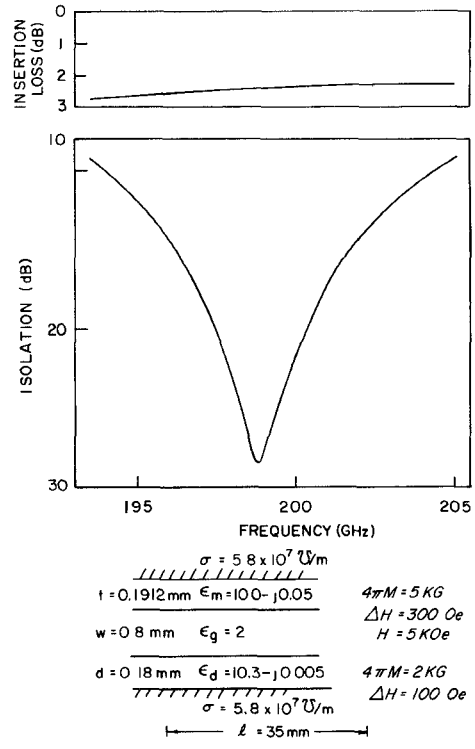

Fig. 16. The frequency characteristic of a double-ferrite isolator.

nonreciprocity in the propagation constant is enhanced in this configuration, and the isolator property can be improved. In fact, the difference of propagation constants in two opposite directions becomes almost the sum of those for the individual ferrite guides. Calculating with essentially the same structural parameters, as in Fig. 12, we have obtained the frequency characteristic shown in Fig. 16. The only parameter we modified is the thickness of Guide 2 in order to keep degeneracy around 200 GHz. It is seen that the insertion-loss characteristic for this structure is almost the same as the one shown in Fig. 14. This is because the loss comes mostly from the main guide in these rather long isolators, as shown in Fig. 15. An increase of nonreciprocity reduces only the "structural loss," which has a minor contribution in this case. Therefore, the most effective use of this ferrite–ferrite configuration is in fabricating a shorter isolator.

We will now investigate possibilities of obtaining an isolator with a shorter length. We recognize that realization of the absorptive coupled-mode isolator requires a sufficiently large loss in the ferrite guide. Otherwise, the reflection at the truncated ends of the ferrite degrades the isolator characteristics. However, a large loss in the ferrite alone is not sufficient for good performance. When a lossier ferrite is used, the attenuation constant α_2 of the basis mode increases and the coupling in the backward direction becomes weaker. This results in an increase of power in the main guide and in deterioration of isolator characteristics. To compensate for this weak coupling and to introduce large attenuations in both the main and ferrite guides, we need to decrease the separation of two guides. When such an arrangement is made, however, the insertion loss is also increased due to the enhanced coupling in the

forward direction. Therefore, in addition to reducing the separation of two guides, we would also like to increase $|\beta_1-\beta_2|$ in the forward direction so that the increase of the coupling coefficient κ is cancelled and $|\beta_1-\beta_2|/\kappa$ is maintained at a large number.

When the length of the isolator with a ferrite having its saturation magnetization given in Fig. 16 is reduced from 35 to 20 mm, insertion loss of several decibels is generated, as $|\beta_1-\beta_2|$ is not large enough. If we can use a ferrite with a larger saturation magnetization such as 10 kG, the insertion loss may be reduced to about 1 dB by shortening the ferrite to 20 mm.

VII. Conclusions

We proposed a new type of distributed isolators for millimeter-wave applications. The structure is based on the mode-coupling phenomena often employed in the integrated optical circuits. We presented a general mode-coupling theory for the structure containing a gyrotropic (ferrite) waveguide. Qualitative discussions, as well as detailed numerical studies, have been conducted, and a number of practical considerations discussed in designing the isolator at frequencies around 200 GHz.

Appendix
Symmetry Property of D_{ij} and N_{ij}

Since we have

$$D_{ij}=\int \hat{a}_y\cdot\left(\bar{E}_j\times\bar{H}_i^* +\bar{E}_i^*\times\bar{H}_j\right)dS \tag{A1}$$

it is easily shown that

$$D_{ji}^* =\int \hat{a}_y\cdot\left(\bar{E}_i^*\times\bar{H}_j+\bar{E}_j\times\bar{H}_i^*\right)dS=D_{ij}. \tag{A2}$$

Hence, the matrix $[D]$ is Hermitian.

On the other hand, N_{ij} is written as

$$\begin{aligned}N_{ij}&=\beta_j\int \hat{a}_y\cdot\left(\bar{E}_j\times\bar{H}_i^* +\bar{E}_i^*\times\bar{H}_j\right)dS\\&\quad+\omega\int\left[\bar{H}_i^*\cdot\left(\bar{\bar{\mu}}-\bar{\bar{\mu}}_j\right)\cdot\bar{H}_j+\bar{E}_i^*\cdot\left(\bar{\bar{\epsilon}}-\bar{\bar{\epsilon}}_j\right)\cdot\bar{E}_j\right]dS\\&=\omega\int\left(\bar{H}_i^*\cdot\bar{\bar{\mu}}\cdot\bar{H}_j+\bar{E}_i^*\cdot\bar{\bar{\epsilon}}\cdot\bar{E}_j\right)dS\\&\quad+j\int\left[\bar{E}_i^*\cdot\left(j\beta_j\hat{a}_y\times\bar{H}_j+j\omega\bar{\bar{\epsilon}}_j\cdot\bar{E}_j\right)\right.\\&\quad\left.-\bar{H}_i^*\left(j\beta_j\hat{a}_y\times\bar{E}_j-j\omega\bar{\bar{\mu}}_j\cdot\bar{H}_j\right)\right]dS\\&=\omega\int\left(\bar{H}_i^*\cdot\bar{\bar{\mu}}\cdot\bar{H}_j+\bar{E}_i^*\cdot\bar{\bar{\epsilon}}\cdot\bar{E}_j\right)dS\\&\quad+j\int\left(\bar{E}_i^*\cdot\nabla_t\times\bar{H}_j-\bar{H}_i^*\cdot\nabla_t\times\bar{E}_j\right)dS.\end{aligned} \tag{A3}$$

Thus

$$\begin{aligned}N_{ji}^* &=\omega\int\left(\bar{H}_j\cdot\bar{\bar{\mu}}^*\cdot\bar{H}_i^* +\bar{E}_j\cdot\bar{\bar{\epsilon}}^*\cdot\bar{E}_i^*\right)dS\\&\quad-j\int\left(\bar{E}_j\cdot\nabla_t\times\bar{H}_i^* -\bar{H}_j\cdot\nabla_t\times\bar{E}_i^*\right)dS.\end{aligned} \tag{A4}$$

From the relation

$$\begin{aligned}&\int\left(\bar{E}_i^*\cdot\nabla_t\times\bar{H}_j-\bar{H}_j\cdot\nabla_t\times\bar{E}_i^*+\bar{E}_j\right.\\&\qquad\left.\cdot\nabla_t\times\bar{H}_i^* -\bar{H}_i^*\cdot\nabla_t\times\bar{E}_j\right)dS\\&\quad=\int\nabla_t\cdot\left(\bar{E}_i^*\times\bar{H}_j+\bar{E}_j\times\bar{H}_i^*\right)dS\\&\quad=\int\hat{n}\cdot\left(\bar{E}_i^*\times\bar{H}_j+\bar{E}_j\times\bar{H}_i^*\right)dl\\&\quad=\int\left(\bar{H}_j\cdot\hat{n}\times\bar{E}_i^* +\bar{H}_i^*\cdot\hat{n}\times\bar{E}_j\right)dl=0\end{aligned} \tag{A5}$$

the second terms of (A3) and (A4) are shown to be equal. If the material contained in the waveguide is not dissipative, the permeability and permittivity tensor are Hermitian. Hence, the first terms turned out to be equal. These facts prove N_{ij} is Hermitian, as is D_{ij}.

References

[1] Y. Akaiwa, "Bandwidth enlargement of a millimeter-wave y circulator with half-wavelength line resonators," *IEEE Trans. Microwave Theory Tech.*, vol. MTT-22, no. 12, pp. 1283–1286, Dec. 1974.

[2] V. P. Nanda, "A new form of ferrite device for millimeter-wave integrated circuits," *IEEE Trans. Microwave Theory Tech.*, vol. MTT-24, no. 11, pp. 876–879, Nov. 1976.

[3] P. R. McIsaac, "Bidirectionality in gyrotropic waveguides," *IEEE Trans. Microwave Theory Tech.*, vol. MTT-24, no. 4, pp. 223–226, Apr. 1976.

[4] D. Marcuse, "Coupled-mode theory for anisotropic optical waveguide," *Bell. Syst. Tech. J.*, vol. 54, pp. 985–995, May 1975

[5] S. E. Miller, "Coupled wave theory and waveguide applications," *Bell. Syst. Tech. J.*, vol. 33, pp. 661–719, May 1954..

[6] I. Awai and T. Itoh, "Multilayered open dielectric waveguide with a gyrotropic layer," *Int. J. Infrared and Millimeter Waves*, vol. 2, no. 1, pp. 1–14, Jan. 1981.

[7] B. Lax and K. J. Button, *Microwave Ferrite and Ferrimagnetics*. New York: McGraw-Hill, 1962.

Ikuo Awai (M'78) was born in Bujun, Japan, on February 28, 1941. He received the B.S. degree in 1963, the M.S. degree in 1965, and the Ph.D. degree in 1978, all from Kyoto University, Kyoto, Japan.

In 1967, he joined the Department of Electronics, Kyoto University, as a Research Associate, where he has been engaged in research on microwave magnetic waves. From December 1979 to October 1980, he was a Post Doctoral Research Associate at the University of Texas, Austin, on leave from Kyoto University. His current research interests include integrated optics, especially anisotropic thin-film devices.

Dr. Awai is a member of the Institute of Electronics and Communication Engineers of Japan.

Tatsuo Itoh (S'69–M'69–SM'74) received the Ph.D. degree in electrical engineering from the University of Illinois, Urbana, in 1969.

From September 1966 to April 1976 he was with the Electrical Engineering Department, University of Illinois. From April 1976 to August 1977 he was a Senior Research Engineer in the Radio Physics Laboratory, SRI International, Menlo Park, CA. From August 1977 to June 1978 he was an Associate Professor at the University of Kentucky, Lexington. In July 1978 he

joined the faculty at The University of Texas at Austin, where he is now a Professor of Electrical Engineering and Director of Microwave Laboratory. During the summer 1979, he was a Guest Researcher at AEG-Telefunken, Ulm, West Germany.

Dr. Itoh is a member of the Institute of Electronics and Communication Engineers of Japan, Sigma Xi, and Commission B and C of USNC/URSI. He is a Professional Engineer registered in the State of Texas.

Asymptotic High-Frequency Modes of Homogeneous Waveguide Structures with Impedance Boundaries

ISMO V. LINDELL, MEMBER, IEEE

Abstract—**Homogeneous waveguides with both isotropic and anisotropic impedance boundaries are considered and asymptotic high-frequency mode properties are systematically derived. Among the new results are orthogonality properties of the asymptotic HF fields, existence of self-dual solutions, construction of stationary functionals, and an explicit formula for the calculation of the asymptotic attenuation coefficient for the general waveguide.**

I. Introduction

THE PROBLEM of guided waves in structures of large transverse dimensions has many applications, e.g., in antenna feed systems and millimeter and submillimeter wave engineering. A paper on HE_{11} modes in large waveguides was recently published [1]. The theory presented was, however, mainly limited to special geometries and loaded with unnecessary assumptions, which has prompted this author to attempt of a more systematic theory of asymptotic modes.

In the present study, the fields are derived through Hertzian potentials as in conventional waveguide mode analysis [2]. These potentials are expanded in asymptotic series with respect to the inverse powers of the wavenumber k and equations for the coefficients are obtained. The basic is the Helmholtz equation for the two scalar potential functions and the eigenvalue is related to the difference of the propagation factor and the free-space k value. The basic problem is independent of the true impedance properties of the boundary, as was demonstrated in [1]. Properties of the basic solutions are considered, the mode fields satisfy certain orthogonality conditions. Also, the modes are all degenerate. Two functionals are presented that are stationary for the solutions of the basic problem and give the eigenvalue as the stationary value. The eigenvalues are seen to be real so that no attenuation is connected with the basic problem.

Defining two dual transformations, we see that a dual transformation of a basic solution is also a basic solution of the asymptotic waveguide problem. The most natural way, of defining and classifying the mode fields seems to be in terms of two self-dual solutions of the basic problem, because they both satisfy uncoupled boundary conditions. The problem is, then, formulated in terms of one scalar potential function only. A stationary functional is also presented for the self-dual modes. These modes are circularly polarized everywhere, whence there is no need to consider any special coordinate system in the transverse plane. As an application, the circular cylindrical geometry is analyzed for self-dual modes.

The attenuation is obtained in the next problem, which applies the solution of the basic problem. An explicit formula for the calculation of the attenuation coefficient is given. This involves the boundary conditions and is considered separately for an isotropic and an anisotropic boundary. As an example, corrugated surface is analyzed and it is found that the attenuation is decreased if the longitudinal impedance is decreased and the transverse impedance increased, which was demonstrated for special geometries in [1].

II. The Waveguide Problem

The waveguide structure considered here (Fig. 1) is uniform in the z-coordinate and bounded with any closed curve C in the transverse plane. Because of the transla-

Manuscript received February 24, 1981; revised April 30, 1981.

The author is with the Department of Electrical Engineering, Helsinki University of Technology, Otakaari 5A, 02150 Espoo 15, Finland.

0018-9480/81/1000-1087$00.75 ©1981 IEEE